Rapid-to-deploy reconfigurable wireless structural monitoring systems using extended-range wireless sensors

Junhee Kim[1], R. Andrew Swartz[2], Jerome P. Lynch[1]*, Jong-Jae Lee[3] and Chang-Geun Lee[4]

[1]*Department of Civil and Environmental Engineering, University of Michigan, 2350 Hayward Street, 2380 G. G. Brown Building, Ann Arbor, MI 48109-2125, USA*
[2]*Department of Civil and Environmental Engineering, Michigan Technological University, Houghton, MI 49931, USA*
[3]*Department of Civil and Environmental Engineering, Sejong University, 98 Gunja-dong, Gwangjin-gu, Seoul 143-747, Korea*
[4]*Structural Research Team, Expressway and Transportation Research Institute, Korea Expressway Corporation, 50-5 Sencheok-ri, Dongtan-myeon, Hwaseong-si, Gyenggi-do 445-812, Korea*

Abstract. Wireless structural monitoring systems consist of networks of wireless sensors installed to record the loading environment and corresponding response of large-scale civil structures. Wireless monitoring systems are desirable because they eliminate the need for costly and labor intensive installation of coaxial wiring in a structure. However, another advantageous characteristic of wireless sensors is their installation modularity. For example, wireless sensors can be easily and rapidly removed and reinstalled in new locations on a structure if the need arises. In this study, the reconfiguration of a rapid-to-deploy wireless structural monitoring system is proposed for monitoring short- and medium-span highway bridges. *Narada* wireless sensor nodes using power amplified radios are adopted to achieve long communication ranges. A network of twenty *Narada* wireless sensors is installed on the Yeondae Bridge (Korea) to measure the global response of the bridge to controlled truck loadings. To attain acceleration measurements in a large number of locations on the bridge, the wireless monitoring system is installed three times, with each installation concentrating sensors in one localized area of the bridge. Analysis of measurement data after installation of the three monitoring system configurations leads to reliable estimation of the bridge modal properties, including mode shapes.

Keywords: structural monitoring; wireless sensors; modal analysis; smart structures.

1. Introduction

The monitoring of civil structures is an important step in improving the understanding of structural behavior under normal and extreme loads (e.g., earthquakes), as well as illuminating the degradation mechanisms that naturally occur in aging infrastructure systems. Currently, structural monitoring is reserved for special structures (e.g., long-span bridges, hospitals) located in zones of high seismic risk or where strong wind conditions prevail. Even fewer monitoring systems

---

*Corresponding Author, Associate Professor, E-mail: jerlynch@umich.edu

have been deployed for monitoring the health of structures. Market penetration for structural monitoring remains largely limited by the cost and by the complexity of installing wired monitoring systems in large structures. Wireless sensors have been proposed to alleviate the expense and effort required to install a monitoring system. Since the seminal study of wireless structural monitoring by Straser and Kiremidjian (1998), the state-of-the-art in wireless sensing has rapidly evolved with many viable wireless sensing solutions available for reliable structural monitoring (Spencer *et al.* 2004, Lynch and Loh 2006). In addition, many academic groups have showcased the potential role that wireless sensors can play in future structural monitoring systems through field implementations in actual operational bridges. A non-exhaustive set of recent field deployments include wireless monitoring of the Alamosa Canyon Bridge, New Mexico (Lynch *et al.* 2004a), Geumdang Bridge, Korea (Lynch *et al.* 2006), Gi-Lu Bridge, Taiwan (Lu *et al.* 2006), Golden Gate Bridge, California (Pakzad *et al.* 2008) and Wright Bridge, New York (Whelan and Janoyan 2009).

Historically, structural monitoring systems have been viewed as static systems that, once installed in a structure, are rarely changed or modified. This perspective likely finds its origin in the fact that wired monitoring systems are challenging to install and modify. However, wireless sensors eliminate the need for wiring and are therefore easier to install than their wired counterparts. Rapid installation renders wireless monitoring systems very attractive for short-term deployments where response data from operational structures is desired over short periods of time (e.g., hours, days or weeks). For example, short-term monitoring can offer sufficient data from which a rapid condition assessment can be made of an operational bridge (Salawu and Williams 1995). Furthermore, the modularity of the wireless sensors within the monitoring system architecture facilitates relatively easy reconfiguration and modification of the monitoring system topology. Using a small number of wireless sensor nodes, a large number of sensor locations can be achieved.

In this study, a rapid-to-deploy wireless monitoring system is proposed for short-term monitoring of highway bridges. The wireless monitoring system is assembled using a low-cost, low-power wireless sensor node (termed *Narada*) developed for monitoring civil structures as its primary building block. The wireless sensor node features a high-resolution, multi-channel sensing interface, a powerful microcontroller core, and a wireless communication interface. To allow the wireless sensor node to achieve adequate communication ranges appropriately scaled to the dimensions of the structure, a modified version of a standard IEEE 802.15.4 wireless transceiver is fabricated for long-range wireless communications. Specifically, a power amplification circuit is coupled with the transceiver to increase the radio frequency signal by 10 dB. To highlight the utility of a reconfigurable wireless monitoring system, a network of 20 *Narada* wireless sensors are deployed on the Yeondae Bridge, located in Icheon, Korea. The monitoring system is installed and reconfigured twice in order to achieve three different sensor topologies in the structure. The vertical acceleration response of this 180 m steel box girder bridge is monitored during controlled truck loading for each configuration of the wireless monitoring system. With intentional overlapping of the three topologies, the mode shapes of the Yeondae Bridge are obtained during off-line analysis of the wirelessly acquired acceleration response data. The paper is structured as follows: first, the *Narada* wireless sensor node is introduced; second, a modified wireless transceiver for extended-range telemetry is integrated with *Narada* and analyzed during range testing; third, a short-term measurement campaign on the Yeondae Bridge using the proposed wireless monitoring system is presented along with measurement results; finally, the paper concludes with a detailed modal analysis of the bridge conducted off-line using wireless response data.

2. Extended-range wireless sensor for structural monitoring

The *Narada* wireless sensor (Fig. 1) was designed at the University of Michigan for use in smart structure applications including for monitoring and feedback control of large-scale civil structures (Swartz *et al.* 2005). Unlike other application areas, the use of wireless sensors in civil structures requires a low-power hardware design that allows a node to survive for long periods of time (e.g., years) on battery or energy harvesting power sources. The large spatial dimensions of civil structures require large communication ranges in the hundreds of meters. In addition, many civil structures exhibit low amplitude vibrations; high-resolution digitization is therefore necessary to ensure low voltage sensor signals remain well above the quantization error inherent to the analog-to-digital conversion process. Finally, the overall cost of the wireless sensor design should be minimized to ensure that the technology is attractive for commercial adoption. *Narada* has been designed using commercial off-the-shelf embedded system components to achieve a low-power, high resolution wireless sensing and actuation node capable of long-range communication. In comparison to other commercial wireless sensor nodes (e.g., Crossbow Motes, Crossbow iMote and Moteiv Telos), the *Narada* wireless sensor platform offers true, 16-bit analog-to-digital conversion for the digitalization of sensor data, as well as a modular radio design that supports the use of a power amplified IEEE802.15.4 radio capable of communication ranges in excess of 500 m. Another distinguishing feature of the *Narada* wireless sensor node that is beyond the scope of this study is the inclusion of an actuation interface for high speed feedback control of actuators.
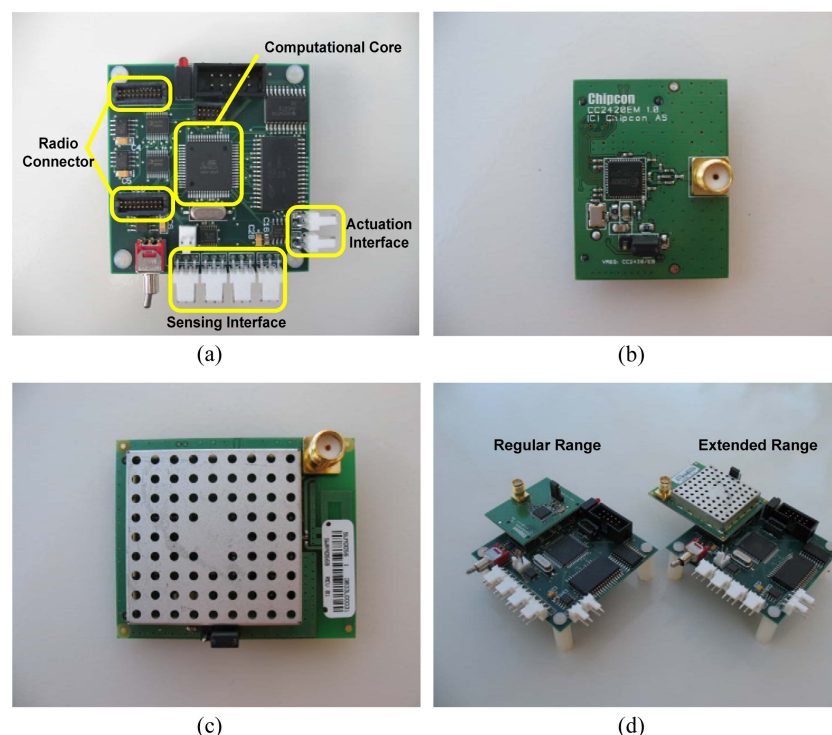

Fig. 1 *Narada* wireless sensor for structural monitoring: (a) main printed circuit board with four functional blocks specified, (b) standard CC2420 transceiver daughter board, (c) power amplified CC2420 daughter board and (d) fully assembled units for regular- and extended-range telemetry

2.1 Narada hardware design

The hardware design of *Narad*a encapsulates the aforementioned functionality necessary for effective operation in structural monitoring applications. In particular, the hardware design of the low-power node is decomposed into four functional blocks that support the node's capabilities to sense, communicate, compute and actuate. (Swartz *et al.* 2005). The first two capabilities (i.e., sensing and communication) replicate the functionality of sensors in the traditional monitoring sensing paradigm. However, the inclusion of computing into the wireless sensor node represents a significant departure from that paradigm since it empowers the wireless sensor node to interrogate raw sensor data individually or collectively with other wireless sensors in a network. In-network data processing (in lieu of communicating high-bandwidth raw data streams) has proven effective in enhancing the reliability of the wireless communication channel while preserving power in battery operated devices (Lynch *et al.* 2004b, Nagayama and Spencer 2007, Zimmerman *et al.* 2008, Rice *et al.* 2008, Kijewski-Correa and Su 2009, Jones and Pei 2009). More recently, it has been proposed that wireless sensors leverage their computational capabilities for service as a controller in real-time feedback control systems (Swartz and Lynch 2009). To achieve this goal, the capability to command actuators has emerged in the design of some wireless sensor prototypes proposed for smart structure applications.

For data collection, *Narada*'s sensing interface is designed around the Texas Instruments ADS8341 analog-to-digital converter (ADC). This ADC supports high data rate collection (maximum 100 kHz) simultaneously on four independent sensing channels (Texas Instruments 2003). The ADS8341 was chosen for the *Narada* design for two reasons. First, it has a high 16-bit digital resolution that is suitable for ambient structural vibration measurements. Second, the ADC can be programmed to collect four channels of single-ended inputs or as 2-channels of differential inputs. While a large fraction of sensors used for structural monitoring are single-ended, some sensors recently proposed for structural monitoring (e.g., the Silicon Designs SD2012 accelerometer) offer superior performance when utilized in differential output mode (Silicon Designs 2009). After data is collected by the sensing interface, it is passed to the computational core consisting of an embedded microcontroller (Atmel ATmega128) and memory. The Atmega128 is a low-power, 8-bit microcontroller with 128 kB of flash memory (for the storage of programs), 4 kB of electrically erasable programmable read-only memory (for the storage of program constants) and 4 kB of static random access memory (for the storage of sensor data). To enlarge the amount of memory available for the storage of sensor data, an additional 128 kB of external static random access memory is included in the sensor design. The physical circuit corresponding to the computational core and sensing interface are combined on the same 4-layer printed circuit board (Fig. 1(a)). While beyond the scope of this paper, a 2-channel, 12-bit digital-to-analog converter (Texas Instruments DAC7612) is also included in the *Narada* circuit board to serve as an actuation interface. The *Narada* actuation interface has been previously utilized during wireless structural control studies (Swartz and Lynch 2009). The printed circuit board (PCB) has been carefully designed to ensure digital circuitry (e.g., microcontroller or memory) and its associated noise does not contaminate the performance (i.e., reduce the effective resolution) of the ADC. The PCB design preserves almost the full 16-bit ADC resolution with the quantization error measured to be slightly greater than one bit (i.e., ADC's resolution is estimated to be about 15-bits which corresponds to a quantization error of 0.15 mV relative to the 0-5V input voltage range of the ADC).

2.2 Modular radio boards for short- and extended-range telemetry

The performance of the wireless structural monitoring system is directly correlated to the performance of the wireless transceivers utilized for communication in the system. While a plethora of transceivers have been previously integrated with various commercial and academic prototypes (Lynch and Loh 2006), the field appears to be converging on transceivers that comply with the IEEE 802.15.4 radio standard. This standard defines a physical (PHY) and medium access control (MAC) protocol layer for low-power short-range wireless personal area networks (WPAN) such as sensor networks (IEEE 2006). In the design of *Narada*, the popular Texas Instruments CC2420 IEEE 802.15.4 transceiver is selected (Texas Instruments 2008). The CC2420 operates on the 2.4 GHz band at 250 kbps using direct sequence spread spectrum (DSSS) radio frequency modulation techniques. The transceiver is obtained from the vendor on its own printed circuit board; this daughter board (Fig. 1(b)) can be easily connected to the main *Narada* circuit board (Fig. 1(d)).

A particularly useful feature of the CC2420 transceiver is that the output wireless signal can be easily varied from weak to strong; signal strength is set by writing to an internal hardware register on the CC2420. Allowing the user to set the wireless signal strength is a powerful feature of the CC2420. In effect, an end-user can balance communication range and power consumption of the radio. For example, eight discrete levels of radio strength can be selected ranging from 0 to -25 dB. The power consumption of the radio when using a signal strength of 0 dB (long-range) is 57.4 mW. In contrast, when configured to use a signal strength of -25 dB (short-range), the radio only consumes 28 mW. The discrete levels of radio strength and their corresponding power consumption characteristics during transmission are plotted in Fig. 2. It is difficult to prescribe a precise range to each of these output signal strengths since communication range is a function of the output power, antenna type, antenna location, as well as many other environmental parameters (Bensky 2004). However, under favorable conditions, an output power of -25 dB would offer short communication ranges (10's of meters) while a 0 dB power level could achieve ranges in excess of 100 m.

In civil engineering applications, the size of the instrumented structure often necessitates that data be transmitted distances in the hundreds of meters. Therefore, the short communication range
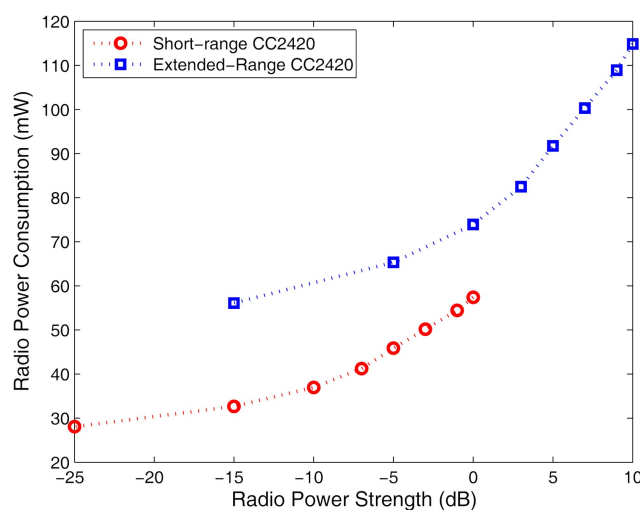

Fig. 2 CC2420 power consumption during transmission for discrete levels of radio signal strength

offered by the standard CC2420 transceiver could require the deployment of a multi-hop wireless sensor network in which data is "hopped" from node-to-node until it reaches its intended recipient. However, the redundant data transmission in multi-hop networks consumes precious communication bandwidth thereby limiting the effective throughput of the network as a whole (Raghavendra *et al.* 2004). Where data throughput is critical, bandwidth may be recovered by increasing the transmission range of individual units. Increased range can be achieved by increasing the transmitted signal strength. One means of increasing signal strength is to adopt specialized antennas such as high-gain, directional antennas where the signal is concentrated in a radio frequency (RF) beam oriented in a specific direction. Another approach is to amplify the signal output.

In this study, a power-amplified CC2420 transceiver circuit (Fig. 1(c)) fabricated to fit the *Narada* radio interface is adopted (Grini 2006). This extended-range transceiver amplifies the CC2420 output signal by 10 dB using a power amplifier circuit between the CC2420 chip and the antenna connector. In the United States, the power amplified CC2420 operates below the Federal Communications Commission (FCC) maximum permissible power level of 1 W. To achieve the 10 dB gain in signal strength, the power-amplified circuit consumes twice the current of the standard CC2420 transceiver board when transmitting. The radio strength of the extended-range radio and its corresponding power consumption characteristics when transmitting are plotted in Fig. 2. When the extended range radio is idle, the power amplification circuit only draws 6 mW of power. The short-range and extended-range radios are modular components that can be swapped using the same underlying *Narada* circuit board as shown in Fig. 1(d). This design approach allows the end-user to select the CC2420 transceiver board that best meets their range requirements and energy budgets (in the case of battery operated devices).

2.3 Embedded software design

An embedded operating system has been custom written for the *Narada* wireless sensor node. The role of the operating system is to simplify the operation of the wireless sensor for end-users and to provide an intermediate software layer between hardware and upper software written for data interrogation. Data acquisition (DAQ) modules have been written for the embedded operating system to provide *Narada* with the capability of real-time continuous data streaming or buffer-burst data transfer. The DAQ package included in the embedded operating system is written to collect data from the node ADC and to wirelessly transmit the data to a desired location including to a laptop personal computer (PC) serving as a remote data repository. In this study, a centralized PC will be utilized to coordinate the activities of the wireless monitoring system and to serve as a single repository of network measurement data. A text file containing DAQ parameters is created by the user, processed by an executable server program running on the PC, and wirelessly transmitted to the network over a CC2420 development board connected to the PC serial port. This text file includes parameters such as mode of operation (continuous data streaming versus buffer-burst data transfer), identification numbers of the *Narada* nodes to use, *Narada* ADC sensor channels to use, sampling frequency (up to 10 kHz), sensing duration (dependent on sampling rate), and number of samples to buffer locally before transmitting in the buffer-burst mode of operation (up to 30,000 samples).

There are practical limitations on the total number of sensing channels that may be included in a network designated to run in the continuous data streaming mode. In effect, the wireless sensor network is limited by the available bandwidth on a specific channel of the IEEE 802.15.4 radio

spectrum (2.4 GHz). Access to the shared wireless channel is controlled by a time-division multiple access (TDMA) scheme in which each sensor is queried by the server at a specified time for data locally stored in its memory bank. Once data is successfully transmitted, it can be overwritten by the node. However, this method is only reliable if the server has sufficient time to collect locally buffered measurement data before the memory bank fills to capacity. Hence, the server can determine before data collection if, for a given number of sensor channels in the monitoring system and a given sample rate, the network has enough time to collect data from each node before the local data buffer must be overwritten. If the server determines *a priori* that there is a risk of losing data (due to too many channels collecting data at too fast of a sampling rate), it will stop the data collection process and alert the end user. For example, the system sampling at 100 Hz will only be able to collect data from 15 sensor channels before data transmission between the wireless sensors and the PC would require more time than the time it takes to completely fill the local memory at the sensor nodes. To increase the total number of sensor channels in the monitoring system, one approach is to divide the network of *Narada* nodes into separate channels in the 2.4 GHz spectrum (16 are available); each channel can then be concurrently serviced by the PC using separate receivers (Swartz *et al.* 2009). In buffer-burst mode, the PC commands the network of wireless sensors to collect a fixed number of data points, store the data in memory (up to 60,000 data points) and stop data collection. The PC server then would query each sensor one at a time to retrieve measurement data locally stored after data collection has ceased. In this approach, there is no theoretical limit on the number of channels that can be collected at one time by the monitoring system.

Another challenge inherent to wireless sensing is time synchronization of individual nodes operating in the wireless network (Raghavendra *et al.* 2004). Unlike in traditional wired monitoring systems where a single ADC is used in a multiplexed fashion to sample multiple sensor channels, a wireless sensor network is composed of multiple ADCs each being timed by a local clock. Precise time synchronization of the independent clocks must take place using the communication media and will be dependent upon the propagation and processing of synchronization messages broadcast between wirelessly networked nodes. Errors in synchronization between data streams lead to corruption of the phase information contained in the data signals. This can adversely affect the accuracy of some processing algorithms commonly associated with modal analysis (Ginsberg 2001), input-output or multiple-output modeling (Lei *et al.* 2005), or feedback control (Lian *et al.* 2005). This task is made more difficult in wireless networks where signal propagation times are stochastic and direct communications between all units in the network may not be possible (Raghavendra *et al.* 2004). Only recently have elegant strategies for accurate time synchronization have been reported (Nagayama and Spencer 2007, Yan *et al.* 2009).

In the embedded operating system of *Narada*, time synchronization is achieved through the use of beacon signals. Prior to data collection, the *Narada* wireless sensors in the monitoring system are notified of a pending data collection request. Upon receipt of this notification, each node goes into standby mode waiting to receive a beacon packet from the PC. Assuming receipt of the beacon packet occurs at the same time in all of the nodes, a start time is established and the data collection process initiated. However, small synchronization errors can result from beaconing due to different signal propagation times and different processing times. The differential signal propagation times are stochastic, but are limited by the signal propagation range of the system. For example, if a node is 1 km from the PC server, the time for the beacon to travel (based on the speed of light) is as large as 3.3 μs (a rather negligible number when considering the fact that sampling frequencies in structural monitoring systems are generally less than 1 kHz). More significant is the differential processing
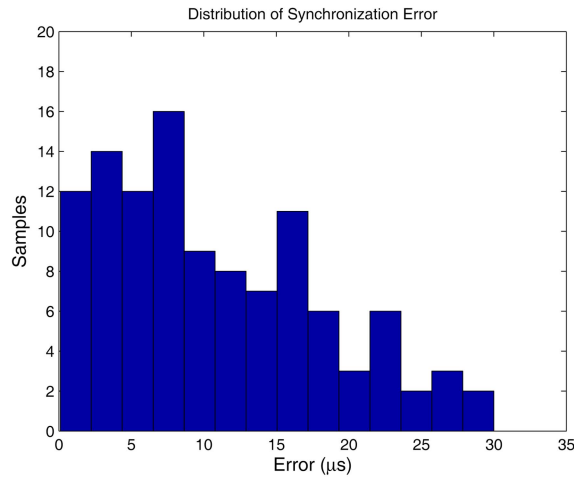
Fig. 3 Histogram of the measured differential beacon time synchronization errors experimentally obtained in a *Narada* wireless sensor network (a total of 111 samples collected)

time. The synchronization error from differential processing can be minimized by limiting the actions of the wireless sensors prior to the start of a data collection run. In *Narada*, the node is placed in a wait state (composed of a "while" loop) that repeats the execution of four assembly instructions. The wait state stops when the PC server's beacon packet is received and serviced. This practice limits the differential processing time to at most, four clock cycles on the Atmega 128 microcontroller plus any delays in processing packets in the CC2420 transceiver.

Since the time synchronization error is stochastic, it must be experimentally quantified. The synchronization error due to differential processing time has been characterized experimentally by use of multiple, collocated sensing nodes programmed to raise a digital logic line when the first data point is ready upon reception of the system start beacon. The differential processing time is then measured on a digital oscilloscope during repeated measurements. The differential processing time synchronization error on Narada is found to be a Poisson distribution with a mean of 7.4 μs, and peak observed value of 30 μs. The distribution of these errors is depicted in Fig. 3. Considering 200 Hz as a typical sampling frequency for civil engineering applications, these results indicate a maximum synchronization error of less than 1 % of a typical time step on the *Narada* system.

3. Performance assessment of the extended-range wireless transceiver

The performance of the extended-range IEEE 802.15.4 wireless transceiver is quantified by conducting range testing in an outdoor paved lot. Special embedded software is written for the *Narada* wireless sensor node where one wireless sensor transmits data packets that are then received by a PC server. The strength of the *Narada* radio signal is recorded using the radio signal strength indicator (RSSI) field that is appended to each packet header received by the transceiver. To understand how the performance of the radio varies as a function of range, the test is repeated with the wireless sensor placed at varying distances away from the PC server. A total of four tests are conducted using a *Narada* wireless sensor node placed 50 cm above the surface of the ground:

i. A *Narada* wireless sensor node with a standard-range IEEE 802.15.5 transceiver integrated is used during range testing. An omni-directional swivel antenna (Antenova Titanis) is used as the radio's primary antenna.

ii. A *Narada* wireless sensor node with an extended-range IEEE 802.15.5 transceiver integrated is used during range testing. An omni-directional swivel antenna (Antenova Titanis) is used as the radio's primary antenna.

iii. A *Narada* wireless sensor node with a standard-range IEEE 802.15.5 transceiver integrated is used during range testing. A directional antenna (D-Link DWL-M60AT) is used as the radio's primary antenna.

iv. A *Narada* wireless sensor node with an extended-range IEEE 802.15.5 transceiver integrated is used during range testing. A directional antenna (D-Link DWL-M60AT) is used as the radio's primary antenna.

First, the omni-directional antenna is used with the standard- and extended-range IEEE 802.15.4 transceivers. The omni-directional antenna radiates RF energy in all directions from the *Narada* wireless sensor node. The test results are plotted in Fig. 4(a); the signal strength of the standard-range radio drops quickly at around 200 m with communication failures experienced. However, the extended-range radio operates at 300 m due to enhanced signal strength. Next, the directional antenna is used with *Narada* nodes with the standard- and extended-range radios integrated. The directional antenna concentrates the RF energy into a specific beam direction; the concentration of RF energy in a single direction should result in higher RSSI measurements along with greater communication ranges. Fig. 4(b) shows the results focusing on data above 250 m. The signal strength of the extended-range radio is roughly 10 dB greater than that of the standard-range radio. It can be concluded that the communication range of the standard-range radio is around 500 m. However, performance range of the extended-range radios is expected to be more than 600 m.

In general, the 10 dB gain achieved by the extended-range radio results in at least 100 m of additional range for the case of both antennas (omni-directional and directional). However, it should be noted that this added range does come at the cost of increase power consumption by the radio. When maximum communication range is necessary, the range tests reveal that the best antenna to use with *Narada* is a directional antenna. While impressive communication ranges are achieved with a
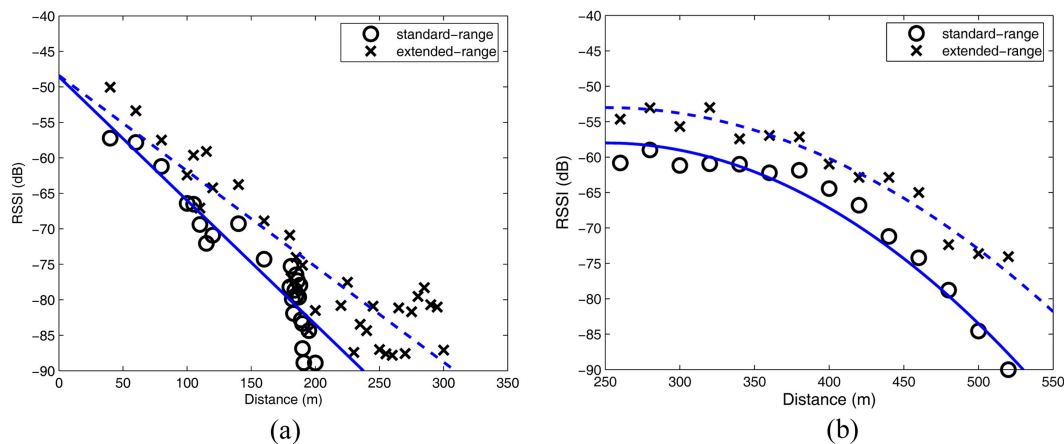

Fig. 4 Range testing of the *Narada* wireless sensor: (a) RSSI of the standard- and extended-range radios using an omni-directional antenna and (b) RSSI of the standard- and extended-range radios using a directional antenna

directional antenna, the wireless sensor node is only capable of communication in one direction. While acceptable in a hub-spoke network architecture, directional communication is less attractive in multi-hop mesh network architectures.

4. Validation of the reconfigurable wireless monitoring system on the Yeondae Bridge

To validate the performance of a reconfigurable wireless monitoring system designed from *Narada* wireless sensors, full-scale dynamic testing is conducted on an operational highway bridge. The Yeondae Bridge, located in Icheon, Korea, is selected. The monitoring system is installed and reconfigured multiple times during forced vibration testing of the bridge using a calibrated truck.

4.1 Yeondae Bridge, Korea

The Korea Expressway Corporation (KEX) has constructed a 7.7 km test road along the Jungbu Inland Highway in the vicinity of Icheon, Korea. The test road is a redundant section of the two lane southbound Jungbu Inland Highway that can be opened and closed to highway traffic. The test road was constructed to monitor the behavior of concrete and asphalt pavement systems designed using Korean design codes under normal truck loads (Lee *et al.* 2004). A combination of strain gages, soil pressure sensors and thermocouples are installed along the length of the test road; in total, 1897 sensors are installed within the test road. Along the length of the test road are two medium-span highway bridges (i.e., Geumdang and Yeondae Bridges) and one short-span highway bridge (i.e., Samseung Bridge). Despite the existence of the pavement monitoring system along the test road, the bridges are not instrumented with sensors. Rather, the KEX has partnered with the
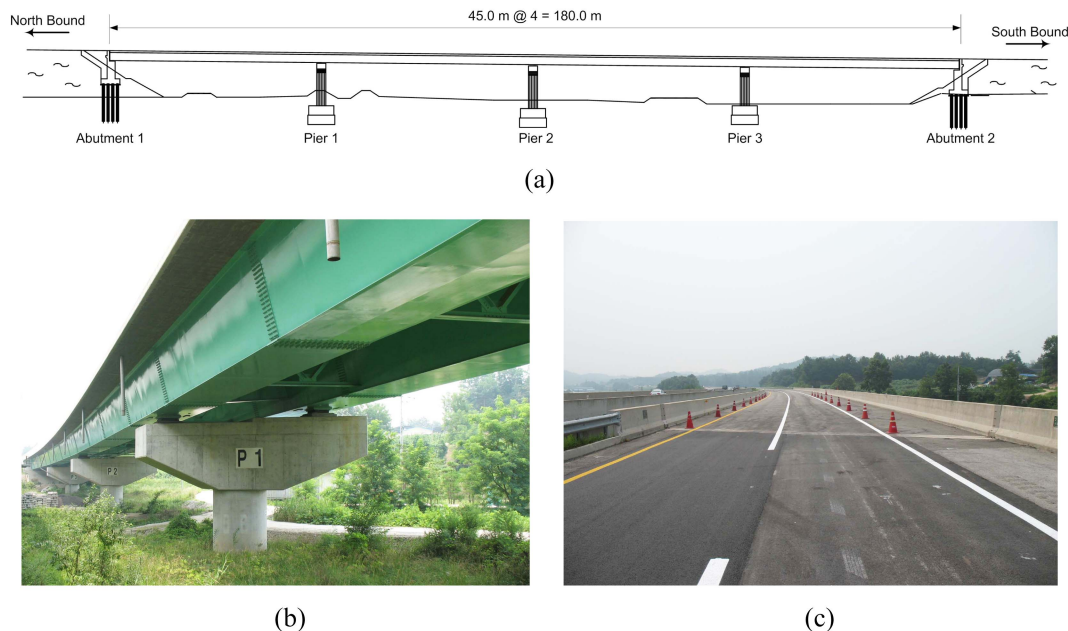

Fig. 5 Yeondae Bridge: (a) profile schematic of the bridge, (b) perspective view at the northern abutment (the curved plan is evident) and (c) view at the top road surface

Smart Infrastructures Technology Center (SISTeC) to experiment with emerging structural health monitoring (SHM) technologies on the test road bridges. A large number of studies focused on the installation of sensors on the three highway bridges have been reported (Lee *et al.* 2004, Lynch *et al.* 2006, Lee *et al*. 2007, Koo *et al.* 2008).

Of the three bridges available, the Yeondae Bridge (Fig. 5) is selected for validation of the reconfigurable wireless structural monitoring system. The bridge is 180 m long and is slightly curved at one end (with a radius of curvature of 1718 m). Along the length of the bridge are three concrete piers that divide the bridge into four identical spans, each 45 m long. To accommodate vehicles driving along the curved sections of the bridge, the road has a varying cross-sectional slope from 2.75% to 4%. The bridge also has a large skew angle of 40º at both ends.

The cross section of the bridge consists of two partially-closed trapezoidal steel box girders. The boxes are 2.2 m tall with top and bottom widths of 3.1 m and 2.1 m, respectively. The concrete deck is 27 cm thick and is designed to act in composite action with the steel box girders. The design of the top flange of the steel box girder varies depending on the flexural moment imposed on the section. At the middle of each span where positive bending moment occurs, the steel box girders are open at their tops, a detail that forces the concrete deck to take the full compressive stress of the bridge section. In contrast, the steel box girders are closed on the supports in order to impose the tensile stress to the top flange of the girder rather than in the concrete deck. The Yeondae Bridge is the first example of a partially-open steel box girder bridge in Korea. Due to the unique geometric and structural design features of the Yeondae Bridge, it is anticipated that the bridge will exhibit unique modal properties. To accurately identify these modal properties, a dense instrumentation of vibration sensors will be required during monitoring of the bridge.

4.2 MEMS accelerometers and signal conditioning

To measure the vertical acceleration of the bridge, two different types of microelectromechanical system (MEMS) accelerometers are adopted for integration with the *Narada* wireless sensor nodes: 14 Crossbow CXL02 accelerometers and 6 PCB Piezotronics 3801D1FB3G accelerometers. Both accelerometers are capacitive-type MEMS accelerometers and are commercially fabricated using standard micromachining methods in a clean-room environment. Compared to other accelerometer types (e.g., piezoelectric or force balanced), these capacitive MEMS accelerometers are relatively low cost, costing $300 or less. The CXL02 accelerometer has an acceleration range of ±2 g, noise floor of 0.5 mg, and sensitivity of 1 V/g. The 3801D1FB3G is a ±3 g accelerometer with a 0.15 mg noise floor and 0.7 V/g sensitivity. Both accelerometers are powered by 5 V and output an analog voltage signal between 0 and 5 V (with 2.5 V corresponding to 0 g).

The low noise floors associated with both MEMS accelerometers were determined to be slightly below the quantization error inherent to the 16-bit ADC (with an effective resolution of 15-bits). However, amplification of the accelerometer outputs can drastically improve the signal-to-noise ratio of the digitized acceleration signals. In order to overcome the reduced resolution of the 16-bit ADC, the outputs of the MEMS accelerometers were amplified by a factor of 20 using a custom-designed amplification board (Lynch *et al.* 2006, Wang *et al.* 2007). The signal conditioning board also includes a band-pass filter with a pass-band of 0.014 to 25 Hz. The band-pass filter rejects high frequency electrical noise in the sensor output in addition to anti-aliasing the acceleration signals.

4.3 Deployment of the wireless monitoring system

In this study, 20 *Narada* wireless sensors are utilized with one single-axis accelerometer (Crossbow CXL02 or PCB 3801D1FB3G) interfaced to each node. Each accelerometer is mounted directly to the surface of the bridge deck to measure the vertical deck acceleration (see Fig. 6(b)). In order to realize a very dense sensor network along the 180 m long bridge, a reconfiguring strategy was adopted with the system modified twice after the initial deployment. Instead of installing all 20 wireless sensors across the entire length of the bridge, the system is first deployed with a dense instrumentation of sensors (7.65 m separation between each sensor) concentrated along the northern one-third of the bridge span with 10 units on each side of the bridge (Fig. 6(a)). To improve the performance of the wireless communications, each wireless sensor node was placed on top of a 56 cm tall rubber traffic cone with the accelerometer connected to each node via a short shielded wire (Fig. 6(b)).

The main advantages of wireless sensors are their mobility; in this study, this mobility is exploited to facilitate reconfiguration of the monitoring system. After dynamic testing with the first installation, the twenty wireless sensor-accelerometer pairs are relocated to the center sections of the bridge, as shown in Fig. 6(a). Since modal analysis will be conducted using response data collected, four sensor locations are kept the same between the first and second system configurations. This intentional overlap between two separate installations will allow for the bridge response to be compared between separate excitation events and to permit the stitching together of global mode shapes. After
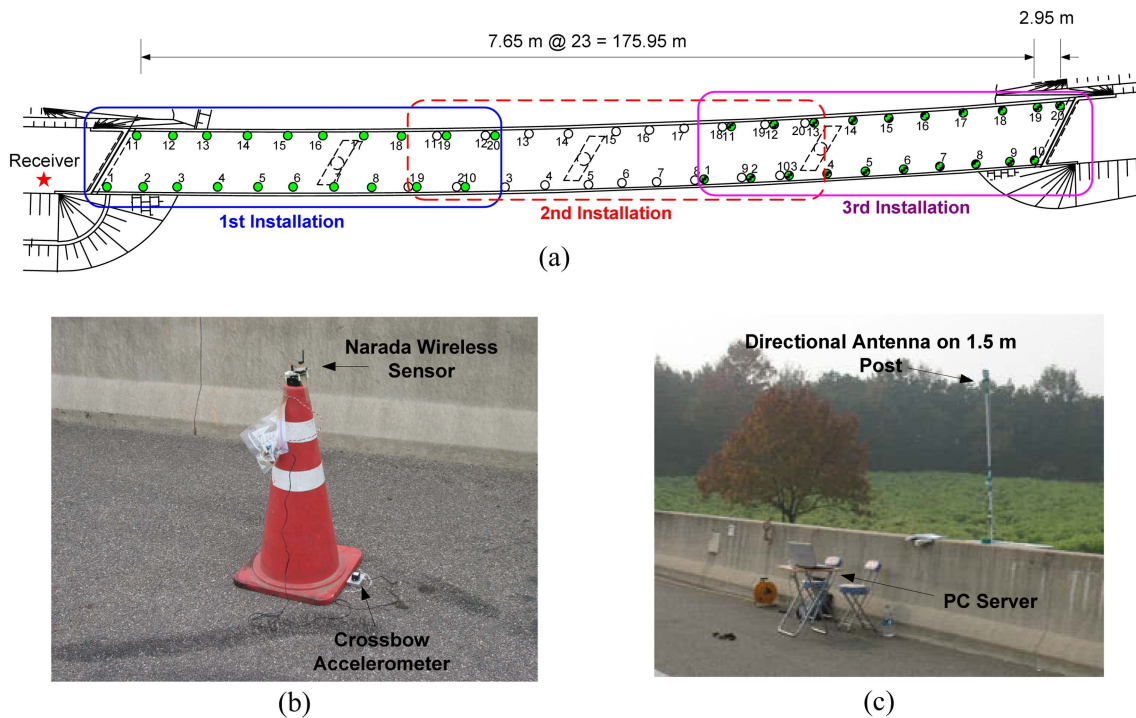

(a)

(b)

(c)

Fig. 6 Wireless monitoring system installed on the Yeondae Bridge: (a) installation of 20 *Narada* wireless sensors in three separate topologies on the bridge, (b) *Narada* wireless sensor with omni-directional antenna installed upon a traffic cone and (c) receiver station with directional antenna installed on a 1.5 m tall post for improved communication performance

data is collected by the second installation, the system is again reconfigured to form a third installation that records the response of the southern-most portion of the Yeondae Bridge (Fig. 6(a)). Due to the absence of cabling work, each sensor installation takes less than one hour to complete. By the end of the test, the reconfiguring strategy adopted results in a dense nodal configuration with wireless sensors installed in 50 different locations along the bridge length.

A receiver (using a directional antenna) is attached to a PC server so that the server can operate the network and collect data from individual wireless sensor nodes deployed along the deck of the bridge. The PC server consists of a laptop computer with a Chipcon CC2420 transceiver attached to its serial port. The PC server is positioned in a fixed location near the northern abutment of the bridge (Fig. 6(c)). This location commands a line-of-sight view of every wireless node on the bridge deck. Reliable communication is anticipated between the receiver and the furthest deployed *Narada* node (which is using a directional antenna and extended-range radio) during the 3rd installation because the maximum communication distance between them is less than the 180 m. During the 1st system installation, sensors closest to the receiver (nodes S1 through S5 and S11 through S14) utilize omni-directional antennas attached to the extended-range radio. For the other sensor locations along the bridge deck, directional antennas are attached to the *Narada* extended-range radio.

4.4 Forced vibration bridge testing

During the time of testing, the KEX closes the test road to regular traffic so that forced vibration testing of the Yeondae Bridge can be conducted using controlled truck loading. Forced vibration tests are conducted using a 3-axle truck (Fig. 7) with a total weight of 25 metric tons (measured at a local weigh station prior to arrival at the bridge site). Considering the fact that truck speed is a key factor in the excitation of bridges (Cantieni 1983), this study explores different truck speeds varied from 30 to 70 km/hr in increments of 10 km/hr (i.e., 30, 40, 50, 60 and 70 km/hr).

For each installation of the wireless monitoring system, the truck is driven over the bridge at each of the five truck speeds. Each time the truck is driven over the bridge, the wireless monitoring system records the vertical acceleration response of the deck at a sample rate of 100 Hz in a buffer-

Fig. 7. Vibrations introduced into Yeondae Bridge using a heavy 3-axle truck driving at constant speeds over the bridge

burst data collection mode. Prior to the truck's entry onto the bridge, the PC server in the wireless monitoring system time synchronizes the nodes and initiates the data collection process by broadcasting a beacon signal. A total of 90 seconds of acceleration data is collected by the wireless monitoring system during each bridge crossing by the truck. The 90 s acceleration time history record collected at each wireless sensor is stored in memory prior to communication to the PC server. With each measurement point 16-bits, the 90 s time history record occupies 18 kB of memory which is only 14% of the memory available on the *Narada* node. Once the data collection task is completed, the central PC server queries each wireless sensor one-by-one for measurement data.

In total, 15 separate dynamic tests are conducted during the measurement campaign on the Yeondae Bridge. Specifically, the truck is driven across the bridge at five different speeds for each configuration of the wireless monitoring system. Fig. 8 presents a typical measured response of the bridge for sensor location S1 through S10 (Fig. 6(a)) for the first sensor network installation. Fig. 8(a) corresponds to the response of the bridge resulting from the truck crossing the bridge at 30 km/hr while Fig. 8(b) corresponds to the truck crossing at 70 km/hr. The wireless monitoring system collects data for 90 seconds which is sufficient to completely capture the response of the bridge regardless of the truck speed. A 30 sec segment of the bridge response to the 70 km/hr truck at sensor locations S1 and S4 in the first system installation is presented in Fig. 9. During data collection, no data loss is encountered revealing the robustness of the wireless communications in the *Narada* wireless sensor network. As can be observed in the time history plots, the acceleration response for each truck crossing is time synchronized with the initiation of bridge response occurring at the same time. As expected, larger levels of acceleration are observed when the truck is driven over the bridge at higher speeds.
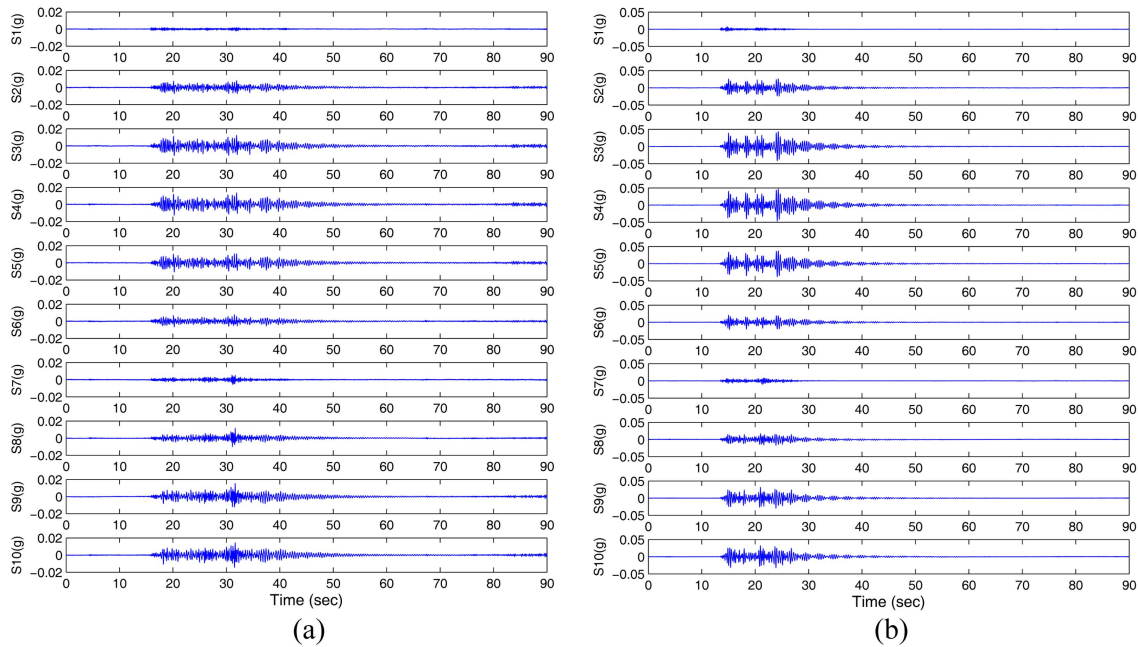

Fig. 8 Acceleration response of the Yeondae Bridge measured at the first sensor installation: (a) 30 km/hr truck speed and (b) 70 km/hr truck speed, sensor number (S1 through S10) corresponds to the number presented in Fig. 6(a)
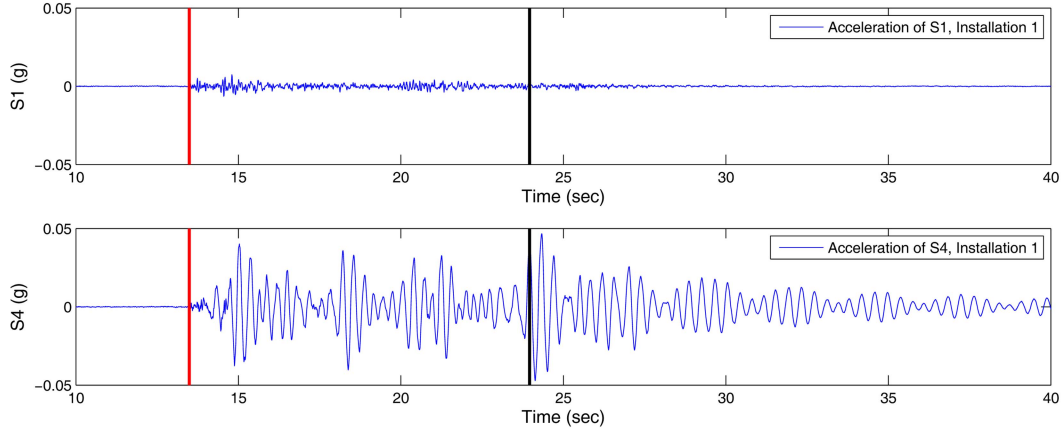
Fig. 9. Acceleration response of the Yeondae Bridge for the 70 km/hr truck at sensor locations S1 (top) and S4 (bottom) in the 1st installation of the monitoring system. The two vertical lines correspond to the point in time when the truck enters and exits the bridge

5. Modal analysis by frequency domain decomposition (FDD)

Modal analysis is conducted on the bridge response data to derive mode shapes. In particular, the FDD method is used in this study, because it is an output-only modal analysis method. While some information is known about the bridge loading (e.g., the weight and speed of the truck), only measurements of the bridge response are available for analysis.

5.1 Frequency domain decomposition (FDD)

FDD is an output-only version of the complex mode indication function (CMIF) method which is a sophisticated frequency domain modal identification method that is capable of accurately identifying the real and imaginary components of closely spaced modes. Output-only system identification is theoretically valid under the assumption of a broadband, white noise input. Broadband inputs excite every vibrational mode of the system with identical intensity due to their infinite frequency bandwidth and constant spectra. Therefore, system identification can still be conducted on broadband excitations despite ignorance of the specific input time history record. Since the early 1980s, the decomposition of output spectra using singular value decomposition (SVD) has been studied (Peeters and Ventura 2003). Shih *et al.* (1988) applied SVD to decompose system frequency response functions (FRF) to identify complex-valued modes using input-output data sets. Later, Brinker *et al.* (2001) reformulated their approach by using the power spectral density (PSD) functions of the system output; the approach was named frequency domain decomposition. The approach offers a robust method of extracting mode shapes of a structure when excited by a broadband excitation source.

The power relationship between the system input, $u(t)$ and the measured output, $y(t)$ can be expressed in the frequency domain as follows

$$G_{yy}(j\omega) = H(j\omega)G_{uu}(j\omega)H^H(j\omega) \qquad (1)$$

where $G_{uu}(j\omega)$ is the power spectral density (PSD) matrix of the input, $G_{yy}(j\omega)$ is the PSD matrix of

the output, $H(j\omega)$ is the FRF matrix of the structural system, and $H^H(j\omega)$ is the complex transpose conjugate of $H(j\omega)$. If the input, $u(t)$ is ideal white noise, then $G_{uu}(j\omega)$ can be considered as constant in an infinite frequency range; hence, the output PSD, $G_{yy}(j\omega)$ directly reflects the product of FRFs, $H(j\omega)H^H(j\omega)$, in other words, the system power characteristics. By using SVD, the output PSD matrix can be decomposed into singular vectors and singular values. It is singular vectors corresponding to large singular values (modal frequencies) that are correlated to the mode shapes of the structure.

5.2 Data partitioning prior to the application of FDD

Some challenges associated with the application of the FDD method are first identified prior to its use for identification of the Yeondae Bridge mode shapes. Specifically, the FDD method is based on the estimated output PSD function which is only valid for a stationary stochastic process. Unfortunately, dynamic bridge testing using a single moving truck does not represent a stationary stochastic process since the truck mass is moving thereby experiencing a non-linear, time-varying coupling with the bridge. However, the free vibration response of the bridge after the truck has left the bridge can be considered as a stationary stochastic process. Thus, in this study the free vibration response of the bridge is used exclusively during modal analysis.

The full time history response collected by the monitoring system is delineated into two portions (i.e., forced and free vibrations). Forced vibrations correspond to the portion of the acceleration time history records of when the truck is on the bridge. After the truck has exited the bridge, the bridge continues to vibrate due to its free vibration behavior. Fig. 9 shows the acceleration time history response of the Yeondae Bridge corresponding to the 70 km/hr truck excitation measured at sensor locations S1 and S4 in the first sensor network installation. In Fig. 9, two vertical lines are superimposed on the time histories to denote the arrival and exit times of the truck on the bridge. Given the location of sensor S1 (it is only 0.55 m away from the expansion joint between the bridge deck and the northern bridge approach), it can be used as a trigger sensor from which the time of the truck first entering the bridge can be identified. It should be noted that because the Yeondae Bridge is supported on elastomeric pads (which act mechanically like low-pass filters isolating vibration from the span surroundings), determination of truck arrival times based on threshold detection should be accurate. The exiting time calculated from the known bridge length and established truck speed is recognized to only be a rough approximation of the exit time of the truck. To proceed with modal analysis, the free vibration response of the bridge well after the estimated exit time of the truck is used as a stochastic stationary process for modal analysis by the FDD method. This approach to partitioning the measured bridge response is executed on the entire data set (i.e., on every data record collected during the 15 separate dynamic tests).

5.3 Application of the FDD method

In this study, the free vibration response of the bridge is used for extraction of the bridge modal frequencies and mode shapes. Before mode shapes can be estimated, the modal frequencies of the bridge must be identified. A peak picking approach for estimation of modal frequencies is adopted. As shown in Fig. 10, power spectral density functions obtained from the free vibration response of two collocated sensors at location S9 (1st installation) and S1 (2nd installation) are plotted. The PSD function calculated for each sensor location was improved by using a Hanning window on the time-history data prior to the use of the fast Fourier transform (FFT) algorithm. In addition, repeated
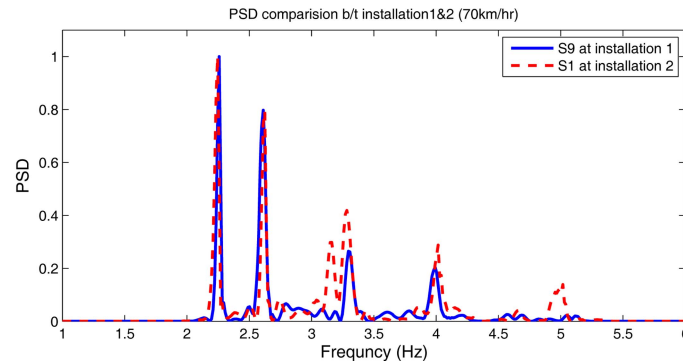
Fig. 10 Power spectral density functions (PSD) at sensor location S9 (1st installation) and S1 (2nd installation) for the free vibration response of the Yeondae Bridge. It should be noted that the two sensor locations are collocated

Fourier spectra calculated from time-history records with 50% time-domain overlap are averaged. This approach to improving the PSD spectra provides a good trade-off between the reduction of noise and the distinctive qualities of the modal peaks (Oppenheim and Schafer 1999). Based on the PSD plots, the first five modal frequencies of the bridge are identified at 2.25, 2.64, 3.34, 4.00 and 4.88 Hz.

Using the estimated PSD functions, the mode shapes of the Yeondae Bridge are estimated by the FDD method for each network configuration. Then, the mode shapes calculated for the three separate network installations are stitched together. Specifically, the local mode shape corresponding to one system installation is scaled (by a scalar constant) relative to the local mode shape of the next installation such that the sum of the differences between the mode shape values at the overlapping nodes is minimized. Fig. 11 depicts the first 5 modes identified (2.25, 2.64, 3.34, 4.00 and 4.88 Hz).

(a)　　　　　　　　　　(b)　　　　　　　　　　(c)
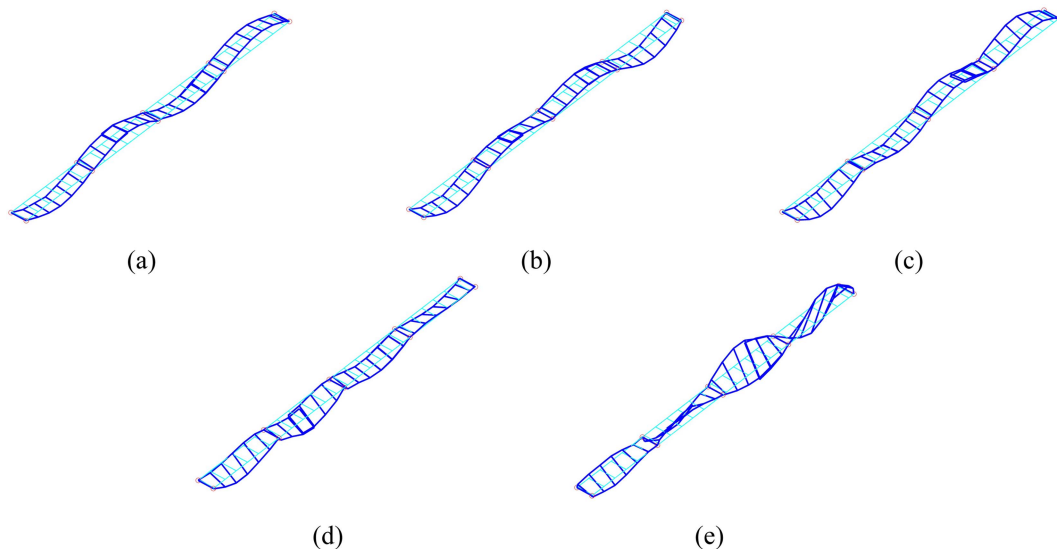
(d)　　　　　　　　　　(e)

Fig. 11 Five estimated mode shapes of the Yeondae Bridge: (a) 2.25 Hz, (b) 2.64 Hz, (c) 3.34 Hz, (d) 4.00 Hz and (e) 4.88 Hz

Of the five modes extracted, the first three modes are pure flexure modes (2.25, 2.64 and 3.34 Hz), the last mode (4.88 Hz) is a pure torsion mode, and the fourth mode (4.00 Hz) is a combined flexure and torsion mode. The first three mode shapes are flexural bending modes that also correspond to modes calculated off-line using a finite element model of the bridge (Kim *et al.* 2009). The fifth mode is a torsional mode that is also in strong agreement with the finite element model. This result proves the quality of the data collected and the accuracy of the off-line modal analysis.

6. Conclusions

In this study, an extended-range *Narada* wireless sensor is proposed for structural monitoring applications. Power amplification of the output of an IEEE 802.15.4 transceiver (i.e., Texas Isntruments CC2420) led to a 10 dB gain in the radio signal strength resulting in improved wireless communications in large-scale structures such as medium-span highway bridges. Twenty extended-range *Narada* wireless sensors are deployed for short time periods on the Yeondae Bridge to measure the bridge acceleration response to truck loading. The mobility of the wireless sensors is leveraged to reconfigure the wireless monitoring system to attain three network configurations that capture the bridge response at 50 different measurement locations. For each of the three network configurations, a 3-axle truck weighing 25 tons is driven across the bridge at speeds ranging from 30 to 70 km/hr. Rapid installation and reconfiguration of the wireless monitoring system is proven to be feasible for short-term monitoring of operational highway bridges. The installation and reconfiguration of the monitoring system took about 1 hour to complete. The performance of the extended-range radio integrated with each *Narada* node proves robust with nearly 100% data delivery rates during three consecutive days of testing. In addition, time synchronization using a beacon approach proves to be accurate. Using the high fidelity acceleration data collected by the wireless monitoring system, off-line modal analysis is conducted including peak picking (to identify modal frequencies) and the use of the frequency domain decomposition method (to identify mode shapes). Reasonable modal frequencies and mode shapes are attained.

This study lays the foundation for future work aimed at deploying *Narada* wireless sensors on highway bridges permanently. Current work is focused on a long-term field deployment study of the extended-range *Narada* wireless sensors on bridges in Korea (such as the Geumdang and Samseung Bridges along the Korean test road) and in the United States. While this study exclusively used accelerometers to measure structural vibrations, future efforts will concentrate on a more heterogeneous array of sensors including accelerometers, strain gages, anemometers, thermometers and linear displacement sensors intended to measure both environmental bridge conditions and bridge responses to load. In addition, the FDD analysis conducted off-line is already embedded in the computational core of the *Narada* wireless sensor for collective computing within the sensor network. The embedded FDD analysis, along with other modal analysis techniques (e.g., stochastic subspace methods), will be executed in-network in future field studies. Accurate mode shape estimation requires the wireless sensor network to be continuously time synchronized during long-term deployments; the issue of clock drift over long periods of operation must be corrected through repeated beacon-based synchronization (as was done in this study). However, more robust long-term strategies for clock synchronization are currently under exploration for embedment in the *Narada* wireless sensor platform.

Acknowledgments

References

Bensky, A. (2004), *Short-range Wireless Communication*, Elsevier, Oxford, UK.

Brinker, R., Zhang, L. and Andersen, P. (2001), "Modal identification of output-only systems using frequency domain decomposition", *Smart Mater. Struct.*, **10**(3), 441-445.

Cantieni, R. (1983), *Dynamic Load Tests on Highway Bridges in Switzerland – 60 years of Experience*, Report 211, Federal Laboratory for Testing of Materials, Switzerland.

Ginsberg, J.H. (2001), *Mechanical and Structural Vibrations : Theory and Applications*, Wiley, New York, NY.

Grini, D. (2006), *CC2420 with External PA*, Application Note 37, Texas Instruments, Dallas, TX.

IEEE (2006), *Standard for Information Technology - Telecommunications and Information Exchange between Systems - Local and Metropolitan Area Networks - Specific Requirements Part 15.4: Wireless Medium Access Control (MAC) and Physical Layer (PHY) Specifications for Low Rate Wireless Personal Area Networks (LR-WPANs)*, Available at http://standards.ieee.org/getieee802/802.15.html.

Jones, J.D. and Pei, J.S. (2009), "Embedded algorithms within an FPGA to classify nonlinear single-degree-of-freedom systems", *IEEE Sens. J.*, **9**(11), 1486-93.

Kijewski-Correa, T. and Su, S. (2009), "BRAIN: a bivariate data-driven approach to damage detection in multi-scale wireless sensor networks", *Smart Struct. Syst.*, **5**(4), 415-426.

Kim, J., Lynch, J.P., Zonta, D., Yun, C.B. and Lee, J.J. (2009), "Modal analysis of the Yeondae Bridge using a reconfigurable wireless monitoring system", *Proceedings of the 10th International Conference on Structural Safety and Reliability (ICOSSAR'09)*, Osaka, Japan, September.

Koo, K.Y., Hong, J.Y., Park, H.J. and Yun, C.B. (2008), "Remotely controllable structural health monitoring systems for bridges using 3.5 generation mobile telecommunication technology", *Proceedings of IABMAS 2008: Bridge Maintenance, Safety, Management, Health Monitoring and Informatics*, Seoul, Korea, July.

Lee, C.G., Lee, W.T., Yun, C.B. and Choi, J.S. (2004), *Development of Integrated System for Smart Evaluation of Load Carrying Capacity of Bridges*, Korea Advanced Institute of Science and Technology, Daejeon, Korea.

Lee, J.J., Fukuda, Y., Shinozuka, M., Cho, S. and Yun, C.B. (2007), "Development and application of a vision-based displacement measurement system for structural health monitoring of civil structures," *Smart Struct. Syst.*, **3**(3), 373-384.

Lei, Y., Kiremidjian, A.S., Nair, K.K., Lynch, J.P. and Law, K.H. (2005), "Algorithms for time synchronization of wireless structural monitoring sensors", *Earthq. Eng. Struct. D.*, **34**(6), 555-573.

Lian, F.L., Moyne, J.R. and Tilbury, D.M. (2005), *Network Protocols for Networked Control Systems, Handbook of Networked and Embedded Control Systems* (Ed. D. Hristu-Varsakelis and W.S. Levine), Boston, MA.

Lu, K.C., Wang, Y., Lynch, J.P., Loh, C.H., Chen, Y.J., Lin, P.Y. and Lee, Z.K. (2006), "Ambient vibration study of the Gi-Lu cable-stay bridge: application of wireless sensing units", *Proceedings of the SPIE - The International Society for Optical Engineering*, San Diego, CA, March.

Lynch, J.P., Law, K.H., Kiremidjian, A.S., Carryer, E., Farrar, C.R., Sohn, H., Allen, D.W., Nadler, B. and Wait, J.R. (2004a), "Design and performance validation of a wireless sensing unit for structural monitoring

applications", *Struct. Eng. Mech.*, **17**(3-4), 393-408.

Lynch, J.P., Sundararajan, A., Law, K.H., Kiremidjian, A.S. and Carryer, E. (2004b), "Embedding damage detection algorithms in a wireless sensing unit for attainment of operational power efficiency", *Smart Mater. Struct.*, **13**(4), 800-810.

Lynch, J.P., Wang, Y., Loh, K., Yi, J.H. and Yun, C.B. (2006), "Performance monitoring of the Geumdang Bridge using a dense network of high-resolution wireless sensors", *Smart Mater. Struct.*, **15**(6), 1561-1575.

Lynch, J.P. and Loh, K.J. (2006), "A summary review of wireless sensors and sensor networks for structural health monitoring", *Shock Vib. Digest*, **38**(2), 91-128.

Nagayama, T. and Spencer, B. F. (2007), *Structural Health Monitoring using Smart Sensors*, NSEL Report Series 001, http://hdl.handle.net/2142/3521.

Oppenhiem, A.V. and Schafer, R.W. (1999), *Discrete-time Signal Processing*, New Jersey: Prentice-Hall Inc.

Pakzad, S.N., Fenves, G.L., Kim, S. and Culler, D.E. (2008), "Design and implementation of scalable wireless sensor network for structural monitoring", *J. Infrastruct. Syst.*, **14**(1), 89-101.

Peeters, B. and Ventura, C.E. (2003), "Comparative study of modal analysis techniques for bridge dynamic characterizes", *Mech. Syst. Signal Pr.*, **17**(5), 965-988.

Raghavendra, C.S., Sivalingam, K.M. and Znati, T.F. (2004), *Wireless sensor networks*, Springer, New York, NY.

Rice, J.A., Mechitov, K.A., Spencer, B.F. and Agha, G.A. (2008), "A service-oriented architecture for structural health monitoring using smart sensors", *Proceedings of the 14th World Conference on Earthquake Engineering*, Beijing, China.

Salawu, O.S. and Williams, C. (1995), "Review of full-scale dynamic testing of bridge structures", *Eng. Struct.*, **17**(2), 113-121.

Shih, C.Y., Tsuei, Y.G., Allemang, R.J. and Brown, D.L. (1988), "Complex mode indication function and its applications to spatial domain parameter estimation", *Mech. Syst. Signal Pr.*, **2**(4), 367-377.

Silicon Designs (2009), *Model 2012 Analog Accelerometer Module*, Data Sheet, Silicon Designs Inc., Issaquah, WA.

Spencer, B.F., Ruiz-Sandoval, M.E. and Kurata, N. (2004), "Smart sensing technology: opportunities and challenges", *Struct. Control Health Monit.*, **11**(4), 349-368.

Straser, E. and Kiremidjian, A.S. (1998), *A Modular, Wireless Damage Monitoring System for Structures*, Blume Earthquake Engineering Center Report No. 128, Stanford, CA.

Swartz, R.A., Jung, D., Lynch, J.P., Wang, Y., Shi, D. and Flynn, M.P. (2005), "Design of a wireless sensor for scalable distributed in-network computation in a structural health monitoring system", *Proceedings of the 5th International Workshop on Structural Health Monitoring*, Stanford, CA, June.

Swartz, R.A. and Lynch, J.P. (2009), "Strategic network utilization in a wireless structural control system for seismically excited structures", *J. Struct. Eng.-ASCE*, **135**(5), 597-608.

Swartz, R.A., Zimmerman, A.T., Lynch, J.P., Rosario, J., Brady, T., Salvino, L. and Law, K.H. (2009), "Hybrid wireless hull monitoring system for naval combat vessels," *Struct. Infrastruct. E.*, under review.

Texas Instruments (2003), *ADS8341 16-Bit, 4-Channel Serial Output Sampling Analog-to-Digital Converter*, http://focus.ti.com/lit/ds/symlink/ads8341.pdf.

Texas Instruments (2008), *CC2420 2.4 GHz IEEE 802.15.4 / ZigBee-ready RF Transceiver*, http://focus.ti.com/lit/ds/symlink/cc2420.pdf.

Wang, Y, Lynch, J.P. and Law, K.H. (2007), "A wireless structural health monitoring system with multithreaded sensing de-vices: design and validation", *Struct. Infrastruct. E.*, **3**(2), 103-120.

Whelan, M.J. and Janoyan, K.D. (2009), "Design of a robust, high-rate wireless sensor network for static and dynamic structural monitoring", *J. Intel. Mat. Syst. Str.*, **20**(7), 849-863.

Yan, G, Dyke, S.J. and Song, W. (2009), "Structural damage localization with tolerance to large time synchronization errors in WSNs", *Proceedings of the 2009 American Control Conference*, St. Louis, MO, May.

Zimmerman, A.T., Shiraishi, M., Swartz, R.A., Lynch, J.P. (2008), "Automated modal parameter estimation by parallel processing within wireless monitoring systems," *J Infrastruct. Syst.*, **14**(1), 102-113.